



Development of an electrochemical biosensor for impedimetric detection of tetracycline in milk

Ayat Mohammad-Razdari¹ · Mahdi Ghasemi-Varnamkhasti^{1,2} · Sajad Rostami¹ · Zahra Izadi^{1,2} · Ali A. Ensafi³ · Maryam Siadat⁴

Revised: 24 April 2020 / Accepted: 30 April 2020 / Published online: 9 May 2020
© Association of Food Scientists & Technologists (India) 2020

Abstract This study dealt with the fabrication of an impedimetric biosensor based on nanomaterial modified with pencil graphite electrode for the detection of tetracycline (TET) in milk samples. For response of the impedimetric aptasensor to be improved, the influence of different parameters (immobilization time of reduced graphene oxide, time of aptamer, and TET binding, and concentration of aptamer) was optimized. In optimum conditions, the aptasensor provided a concentration range

within $1 \times 10^{-16} - 1 \times 10^{-6}$ M and with a limit of detection of 3×10^{-17} M TET. The proposed impedimetric aptasensor was then used in milk samples analysis, and the acceptable recovery was achieved ranging from 92.8 to 102.1%. According to this study, the combination of an aptamer and electrochemical impedance spectroscopy is a promising method for detection of TET in milk samples with high reproducibility and stability.

✉ Mahdi Ghasemi-Varnamkhasti
ghasemymahdi@gmail.com

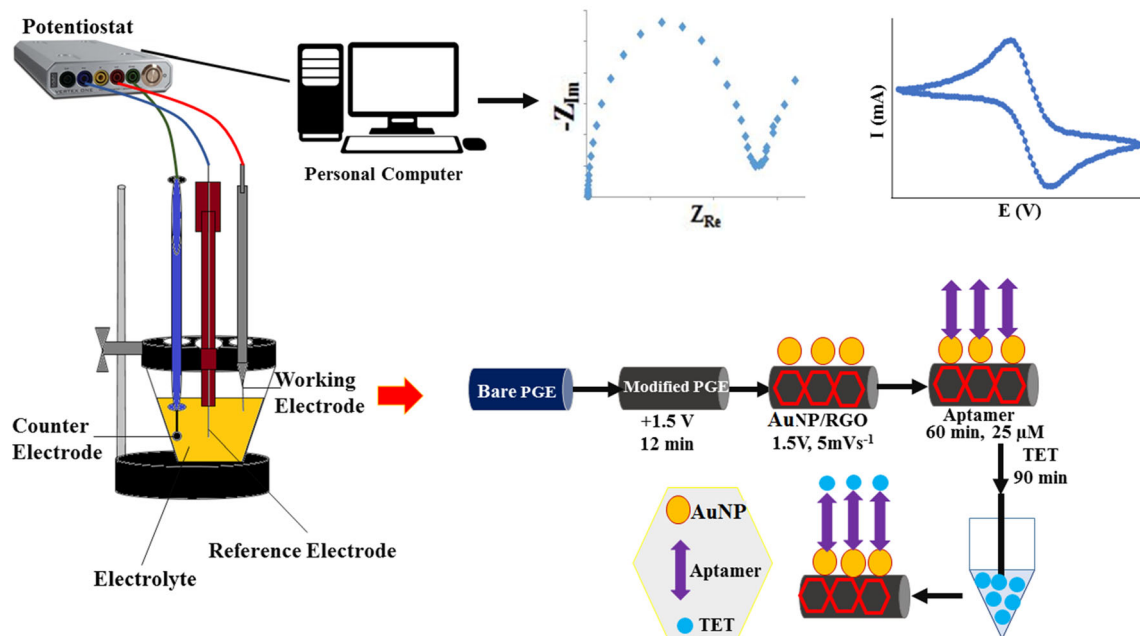
¹ Department of Mechanical Engineering of Biosystems, Shahrekord University, 8818634141 Shahrekord, Islamic Republic of Iran

² Nanotechnology Research Center, Shahrekord University, 8818634141 Shahrekord, Islamic Republic of Iran

³ Department of Chemistry, Isfahan University of Technology, 84156 Isfahan, Islamic Republic of Iran

⁴ LCOMS, Université de Lorraine, EA 7306, 57000 Metz, France

Graphic abstract



Keywords Aptasensor · Antibiotics detection · Nanocomposite · Electrochemical impedance spectroscopy · Reduced graphene oxide

Introduction

Tetracycline (TET) is one of the most conventional antibiotics, which is widely used to treat infectious diseases in veterinary medicine and livestock like mastitis (Ouyang et al. 2017). The overuse of antibiotics such as TET in veterinary medicine as antibacterial and growth enhancer has caused them to remain in food products like e.g., meat, eggs, chicken, and milk (Kim et al. 2010). Food contaminated with antibiotics are a big threat for human and leads to increased drug resistance in the human body (Shen et al. 2014). For food security purposes and preserving consumer health, European Union has determined the maximum residue limit of TET in meat, eggs, and milk to be 220, 440, and 220 nM, respectively (Hou et al. 2015). Therefore, the quantitative and qualitative determination of TET using sensitive, selective, applicable, and specific method in food products such as milk is essential to protect human health.

To date, different methods for detection of TET have been introduced such as spectrophotometry (Palamy and Ruengsitagoon 2017), HPLC (Moudgil et al. 2019), capillary electrophoresis (Moreno-González et al. 2018), liquid chromatography-tandem mass spectrometry (Da Silveira et al. 2018), polymerase chain reaction (Ayeni et al. 2016),

and enzyme linked immuno sorbent assays (Chen et al. 2016). Though these methods are accurate and sensitive, they are laborious, need large and expensive equipment and professional operator. Owing to their high selectivity, low detection limit, cheap and small instrument, portability and no need for professional users, electrochemical aptasensor as a robust alternative to the above-mentioned methods have been developed (Ensafi et al. 2018; Shi et al. 2018).

Aptasensor is known as a sensor based on aptamer activity. Aptamers are known as a new type of recognition targets that have a high ability to bind to different targets, including macromolecules, viruses, and proteins (Benvidi et al. 2018). In comparison with antibodies, aptamers have unique advantages, including small physical size, simple and recyclable synthesis, low-cost, individual three-dimensional (3D) structure and high-thermal stability (Mohammad-Razdari et al. 2019a).

As a two-dimensional (2D) structure of carbon atoms, graphene has unique properties such as electrical conductivity, and mechanical and thermal activities, and as one of the novel nanomaterials it has received lots of attention (Niu et al. 2018). Graphene oxide (GO) is obtained by graphite powder oxidation using strong oxidants such as sulfuric acid and potassium (Ensafi et al. 2018; Tang et al. 2010). Because of the individual electrochemical performance, GO and its related derivatives such as reduced graphene oxide (RGO) have been widely investigated and used in electrochemistry with the aim of modification of electrode surface in electrochemical aptasensors (Song et al. 2016). According to Wu et al. (2017), in comparison

to GO, RGO has better electrochemical efficiency and electrical conductivity in biosensors.

Gold nanoparticles (AuNPs) are ideal for application in electrochemical biosensors due to their excellent electrical conductivity, eco-friendly nature, and good catalyst properties (Tian et al. 2018; Mohammad-Razdari et al., 2019b). The combination of RGO and AuNPs as a nanocomposite, increase electron transfer rate on the electrode surface. Furthermore, it provides more self-assemble sites to connect the aptamer DNA segment (Wu et al. 2017; Zhang et al. 2018).

In this study, for the first time, a pencil graphite electrode (PGE) was selected as a working electrode due to its low price, eco-friendly nature and appropriate mechanical surface, accessibility and simple preparation (Izadi et al. 2016). According to previous reports and to the best of the authors knowledge, this study is the first impedimetric aptasensor based AuNPs/RGO nanocomposite-modified PGE for direct detection of TET. This is the novelty of the work and in this regard, the feasibility of using the aptasensor in real milk samples was investigated. Using electrochemical impedance spectroscopy (EIS) technique, in absence and presence of TET, the value of transfer resistance (R_{ct}) was recorded. According to the results, under the optimum conditions, the proposed biosensor has a good repeatability selectivity, and stability, with a low limit of detection and a wide linear range for TET detection.

Experimental section

Reagents

All of the chemicals used in the work were prepared in analytical grade. All solutions were made in deionized (DI) water. All of materials were purchased from Sigma-Aldrich Company (St. Louis, MO) or Merck Chemicals (Ltd., UK).

A 39-mer thiolated TET-binding aptamer (as a probe) with a sequence (5'-SH-CCCCCGCAGGCCACGGCTTGGGTTGGTCCCACTGCGCG-3') was synthesized in Microsynth AG (Balgach, Switzerland). Using DI water, the oligonucleotide was diluted and stored as a stock solution in a refrigerator ($-20\text{ }^{\circ}\text{C}$). In order to break the disulfide bonds of the aptamer, Dithiothreitol (DTT) was added to the above solution with a ratio of 1:5 (v/v) and kept at room temperature (RT) for 15 min. Then, it was mixed for a few seconds. To remove DTT, ethyl acetate was added to the mixture with an equal volume of the aptamer solution. After that, it was centrifuged at 3000 rpm for 30 s to remove the upper layer. This process was repeated for three times.

Equipment

All electrochemical measurements were performed by Ivium potentiostat/galvanostat with the software of Ivium and a common three-electrode system including a PGE (with 0.7 mm diameter) modified with AuNPs/RGO as a working electrode, an Ag/AgCl (3 M potassium chloride) as a reference electrode, and a platinum wire (with 3 mm length) as a counter electrode was used. All electrochemical experiments for Cyclic voltammetry (CV) and EIS were run in 5.0 mM of $\text{Fe}(\text{CN})_6^{4-/3-}$ in 0.1 M potassium chloride. The experiments were carried out at RT.

Fourier transform infrared spectroscopy (FTIR) (6300 JASCO, Japan) in the range of $400\text{--}4000\text{ cm}^{-1}$ was done to determine the functional groups presence or absence on GO and RGO. Scanning electron microscope (SEM, ZEISS EVO, Germany) was used for the characterization of the electrode at different stages of fabrication.

Synthesis of RGO

Frist of all, based on the modified Hummer's method, grapheme oxide was obtained from natural graphite (Rezaei et al. 2018). Then, 2.5 mg/mL of grapheme oxide suspension was diluted in distilled water and the solution was placed in ice condition. After that, 12.5 g of NaBH_4 was dissolved in 50 mL of water. Then, the solution was slowly mixed to the GO suspension. After that, the suspension was constantly stirred for 12 h at $25\text{ }^{\circ}\text{C}$. At the end, it was filtered to separate RGO and washed with distilled water several times and dried at RT. In order to obtain a homogeneous suspension, 5 mg of RGO was dissolved in 5 mL of DMF.

Aptasensor fabrication

Frist of all, using cyclic voltammetry (CV) method, the working electrode was activated. CV method is a good and common electrochemical method usually used to study redox reactions and electrochemical properties of an analyte in solution that is adsorbed onto the electrode surface (De los Santos Álvarez and Abedul, 2020).

For this purpose, it was treated in 1 M NaOH with scanning potential of 0.0 to $+1.5\text{ V}$, and number cycle of 10. RGO was immobilized on the treated PGE surface by immersing the working electrode (3 mm) into the RGO suspension at RT for 90 min. Then PGE was placed in a PBS (0.1 M, pH 7.0) and CV was performed at -0.10 to $+0.70\text{ V}$ with 10 cycles. AuNPs was immobilized on the electrode surface using corona method electrochemistry. To this purpose, in a 3.0 mM of $\text{HAuCl}_4\cdot 3\text{H}_2\text{O}$ solution CV was run (the potential was scanned from -0.50 V to $+1.5\text{ V}$ with a scan rate of 5 mV/s). The

electrode was then immersed into 0.1 M KNO_3 and the potential was scanned from -0.50 to $+1.50$ V with a cycle of 10 by means of CV.

Due to the self-assembly of thiolated aptamer with AuNPs, it was immobilized at AuNPs/RGO/PGE surface. To do that, by putting the PGE in the aptamer solution, it was immobilized at the surface of AuNPs/RGO/PGE at RT. For remove any unbounded aptamer on the electrode surface, the electrode was then slowly washed with DI water and dried at RT.

TET detection

TET detection was done by dipping the aptasensor into TET solution in optimization time of TET (90 min). After, PGE was then cleaned with DI water for removal of any non-adsorbed antibiotic. Then, EI spectrum was run in a 5.0 mM $\text{Fe}(\text{CN})_6^{4-/3-}$ (in 0.1 M KCl) solution. The R_{ct} value of the proposed aptasensor was used as a response in before and after of TET bounding. Different levels of TET

concentration from 1.0×10^{-16} to 1.0×10^{-6} M were prepared to investigate the aptasensor applicability. In order to depict the calibration plot, ΔR_{ct} versus Log/concentrations of TET was plotted and then EIS signal was used. All experiments were carried out at least three times.

Real sample preparation

Application of the fabricated aptasensor was investigated for TET in different milk samples. Before the actual sample is tested, the milk was diluted at first using phosphate buffer solution (pH = 7) in equal proportions. Milk samples were centrifuged at 24,000 rpm for 45 min to remove additional layers, as the milk contains fat, carbohydrates, and protein. After the milk was centrifuged, three layers of milk were formed. The upper, middle, and lower layers were related to the fat, pure milk, and casein, respectively. Pure milk layer was kept, and then, different concentrations of TET were spiked and the recovery

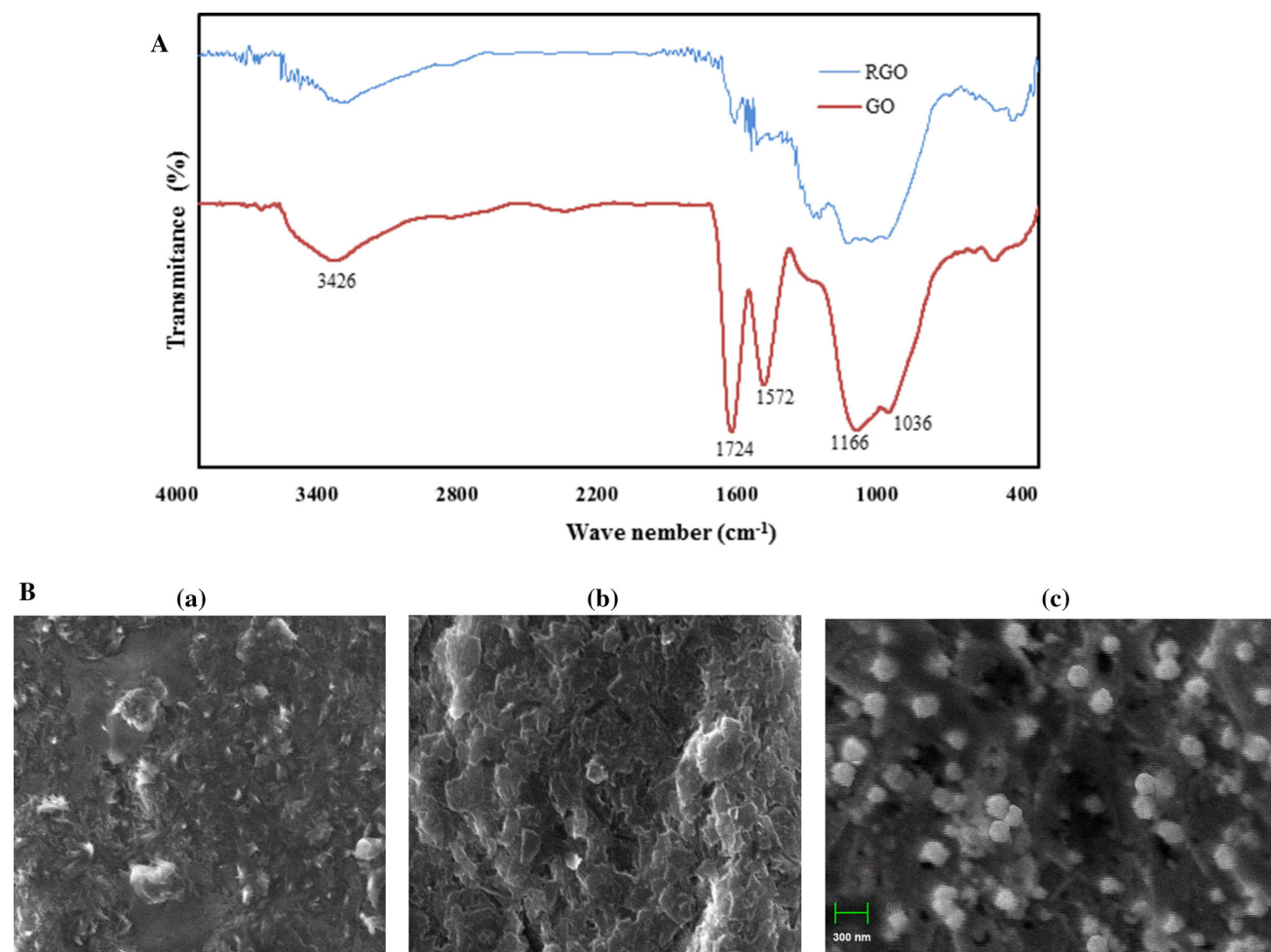


Fig. 1 **A** FTIR spectra of grapheme oxide (GO) and reduced grapheme oxide (RGO) and **B** SEM images of (a) modified PGE, (b) RGO/PGE, and (c) AuNPs/RGO/PGE

percentage was calculated. The above mentioned process was repeated for all samples.

Results and discussion

Characterization of the aptasensor

The functionalization group of GO was more certified using FTIR (Fig. 1A). In the FTIR spectra of the GO nanosheets, the broad absorption band at 3426 cm^{-1} was corresponded to the O–H stretching groups. The intense peaks at 1572 and 1724 cm^{-1} were related to the vibrations of unoxidized graphitic and C = O stretching band in carboxylic acid or carbonyl moieties, respectively (Kassaei et al. 2011). The two absorption peaks at 1166 and 1036 cm^{-1} could be assigned to the C–O stretching vibrations. The reduction of GO was also confirmed by FTIR spectroscopy. As shown in Fig. 1A, all peaks intensities for functional group related to oxygen of RGO were decreased and even some were faded in comparison to the GO peaks intensities. This indicated the successful reduction of GO.

The modified PGE, RGO/PGE, and AuNPs/RGO/PGE morphology was investigated using SEM technique. Figure 1B shows the structures of the modified PGE at various levels (RGO/PGE and AuNPs/RGO/PGE). Figure 1B (a) illustrates the surface morphology of the activated unmodified PGE. As can be seen, the surface of the modified PGE is porous. Figure 1B (b) depicts the RGO layers on the surface of modified PGE, as shown, the RGO layers are clearly visible. Figure 1B (c) exhibits the morphology of AuNPs when it was assembled on the RGO/PGE surface. Overall, AuNPs and RGO were obviously placed on the PGE surface.

CV and EIS were performed for characterization of the aptasensor fabrication interface properties. Figure 2a illustrate the cyclic behaviors of various modified electrodes, at a scan rate of 50 mV s^{-1} . As it can be observed from Fig. 2a (b and c), after the bare PGE surface was coated with RGO and AuNPs, the electron transfer kinetic was increased and the peak current of the electrolyte was also extremely raised (with RGO and AuNPs) in comparison to the unmodified PGE. This occurs owing to the high conduction of RGO and AuNPs and their high effective area surface. Based on Fig. 2a (d and e curves) the peak current of Aptamer/AuNP/RGO/PGE and TET/Aptamer/AuNP/RGO/PGE was reduced compared to the unmodified electrode. This can be explained by the electrostatic repulsion among the negative charge of electrolyte and surface of PGE (Izadi et al. 2016). The peak currents for the unmodified PGE, RGO/PGE, AuNP/RGO/PGE, Aptamer/AuNP/RGO/PGE, and TET/Aptamer/AuNP/RGO/

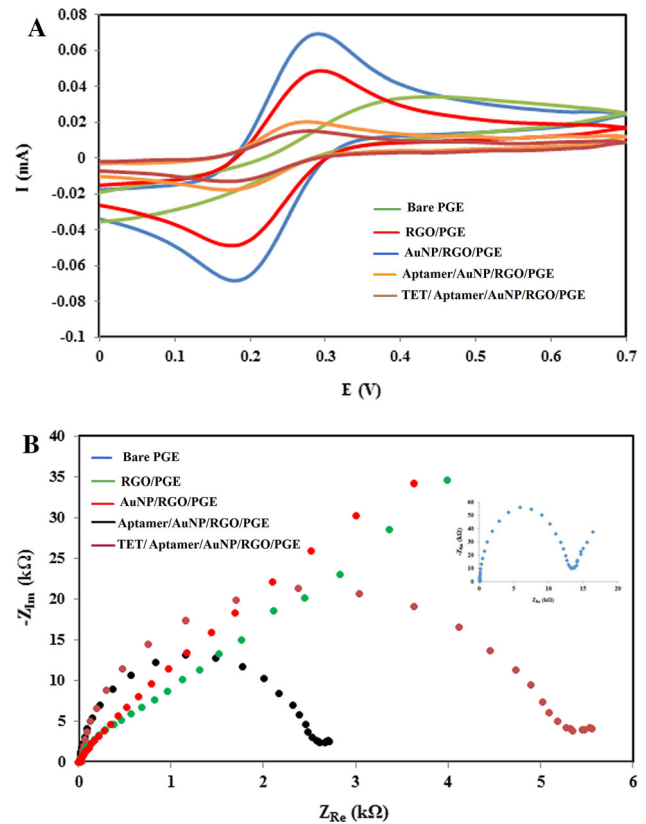


Fig. 2 The CVs (a) and Nyquist plots (b) of different modified electrodes in $5.0\text{ mM Fe(CN)}_6^{4-/3-}$ containing 0.1 M KCl , potential range of -0.1 to 0.70 V with scan rate of 50 mV s^{-1} , Conditions for EIS: the frequency range of 0.01 to 10^5 Hz at the potential of 150 mV

PGE were 0.034 , 0.048 , 0.069 , 0.020 , and 0.015 mA , respectively.

Besides CV technique, EIS was also used to further characterize the different surface of the electrode. EIS is suitable technique for displaying the surface changes of the modified electrodes. The semicircle portion of the Nyquist plot at a higher frequencies is related to the electron-transfer-limited process and the linear part at lower frequency range corresponds to the diffusion process (Wang et al. 2016). As it can be observed from Fig. 2b, after PGE was modified with AuNPs/RGO, the R_{ct} value was reduced compared to the unmodified PGE (Fig. 2b, b and c curves). It occurs because of the high conducting ability and enhances the electron transfer rate in the presence of AuNPs and RGO (Ensafi et al. 2018). As presented in Fig. 2b, curve d, the aptamer immobilization at the AuNP/RGO/PGE surface generated a resistant negatively charge layer at the electrode surface. As a result, the R_{ct} of Aptamer/AuNP/RGO/PGE was increased in comparison to RGO/PGE, and AuNP/RGO/PGE binding between TET and the aptamer leads to a greater increase in the R_{ct} of TET/Aptamer/AuNP/RGO/PGE (Fig. 3b, curve e). It seems to occur due to TET being placed onto the aptamer

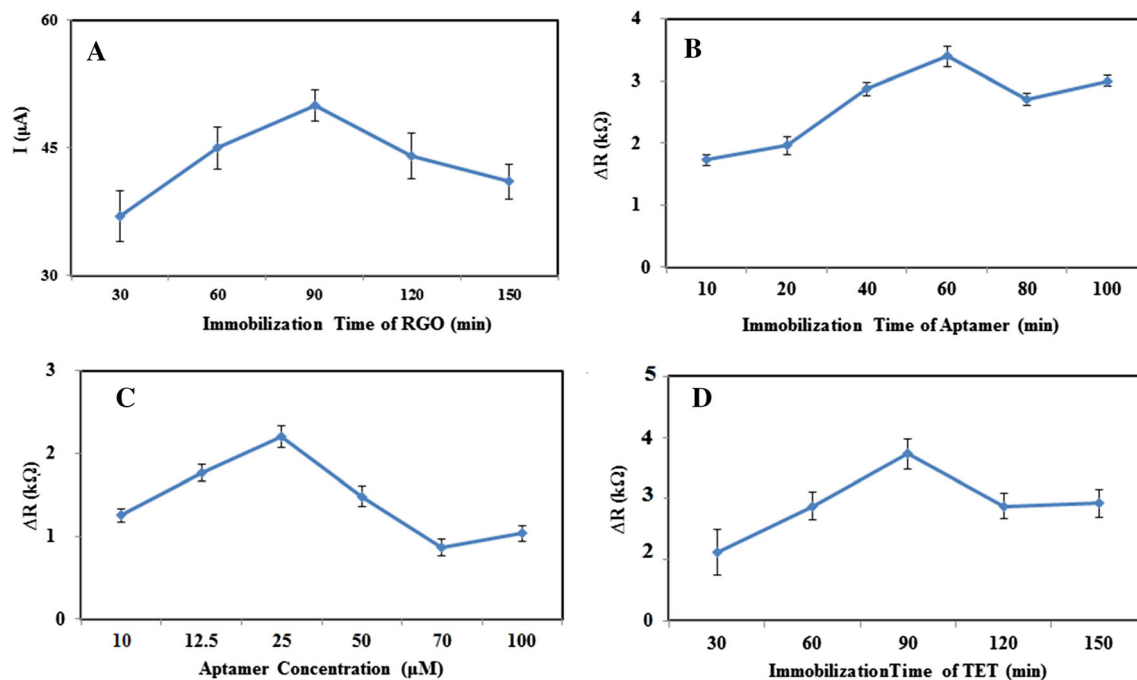


Fig. 3 Influence of **a** immobilization time of RGO on the peak current, **b** immobilization time of aptamer, **c** aptamer concentration and **d** immobilization time of TET on the ΔR_{ct} electrode in 5.0 mM

$\text{Fe}(\text{CN})_6^{4-/3-}$ containing 0.1 M KCl solution. The error bars represented the standard deviation (SD) ($n = 3$)

stands on the electrode surface. These results showed that AuNPs/RGO was effectively attached to the PGE.

Experimental conditions optimization

To access the aptasensor high performance, the RGO immobilization time, the aptamer immobilization time and concentration, and TET immobilization time were optimized. All experiments were carried out in three replicate measurements. To optimize the RGO immobilization time on the treated PGE, the electrode was immersed into the RGO suspension for different times (30, 60, 90, 120 and 150 min) and then, CV was run in the potential of -0.10 to 0.70 V at a scan rate of 50 mV s^{-1} . The results showed that the current was increased and then levelled off as the RGO immobilization time increased up to 90 min. Therefore, 90 min was considered as an optimal immobilization time of RGO (Fig. 3a).

For find the aptamer optimal immobilization time, the working electrode was placed in the aptamer solution (25 μM) for different times (10, 20, 40, 60, 80 and 100 min). Then, EIS was recorded and the R_{ct} was calculated before and after immobilization. The results showed that the ΔR_{ct} was increased and then reduced as the immobilization time was increased up to 60 min. This is probably due to the reason that after 60 min, the surface of AuNP/RGO/PGE were entirely covered by aptamer strands (Benvidi et al. 2018). As shown in Fig. 3b, a time of

60 min was considered for immobilization of aptamer as an optimum choice for the future experiments.

To optimize the concentration of the aptamer, the fabricated biosensor was immersed in the aptamer solution with different concentrations (10, 12.5, 25, 50, 70 and 100 μM) for 60 min. Then, EIS technique was recorded and ΔR_{ct} (R_{ct} before and after aptamer) was measured. According to Fig. 3c, by increasing the concentration of the aptamer up to 25 μM , ΔR_{ct} was increased, and decreased at higher concentrations. At low concentration of aptamer, the AuNP/RGO/PGE surface was not wholly covered by aptamer. Thus, the value of low ΔR_{ct} was achieved for 10.0 and 12.5 μM aptamer. At the concentrations higher than 25 μM , the electrode surface is adequately covered by aptamer strands, so the aptamer immobilization on the AuNP/RGO/PGE surface ΔR_{ct} was declined. Therefore, 25 μM aptamer solution was considered as the optimal concentration for next experiments.

To study the aptasensor detection capability, the interaction time of TET should be studied as one of the important parameters. For this purpose, Aptamer/AuNP/RGO/PGE was immersed into a solution of TET ($1.0 \times 10^{-9} \text{ M}$) for different times (30, 60, 90, 120 and 150 min). The EIS signals were then recorded (before and after addition of TET) and the ΔR_{ct} was calculated. Based on the result, the sensitivity of the biosensor increased and then decreased as the incubation time was increased to

90 min, (Fig. 3d). Thus, 90 min was considered as an optimal time for TET binding.

Performance evaluation of the impedimetric aptasensor

The proposed impedimetric aptasensor was constructed under the optimum experimental conditions and the EIS signals of TET/Aptamer/AuNPs/RGO/PGE were then measured after the addition of different concentrations of TET (Fig. 4a). The EIS method was used for preparation of the calibration curve, by drawing the ΔR_{ct} in before and after the binding between TET *versus*. Log/C. The calibration curve of the fabricated aptasensor showed a linear concentration range from 1.0×10^{-16} to 1.0×10^{-6} M (Fig. 4b) and $\Delta R_{ct} = 0.3274 \text{Log}C_{\text{TET}} + 6.4219$ ($R^2 = 0.9818$) was achieved for TET detection. The limit of detection for TET determination (According to $3.3 \cdot \text{SD}_C/C$, where SD_C denotes the standard deviation for control measurements, and C indicates the slope of calibration curve in the linear range) was calculated to be 3×10^{-17} M.

The Randles circuit was used to fit EIS data as an equivalent circuit including the electrolyte resistance (R_s), R_{ct} , the double layer capacitance (Q), and the Warburg diffusion resistance (Z_w) (inset of Fig. 4b).

The figures of merit of the proposed biosensor are compared with several reported methods for TET detection. As illustrated in Table 1, the limit of detection and the linear concentration range obtained for TET/Aptamer/AuNPs/RGO/PGE are better compared to. previously reported methods.

The aptasensor's repeatability, reproducibility, stability, and selectivity

To investigate the repeatability of the biosensor, an electrode was constructed and placed into a 1.0×10^{-9} M TET and the ΔR_{ct} was measured for five times. Based on the result, the RSD (relative standard deviation) value of 4.2% was achieved. This value of the RSD denotes that the repeatability of the TET/Aptamer/AuNPs/RGO/PGE electrode is acceptable.

The reproducibility of the impedimetric aptasensor was investigated too. For this purpose, five separate aptasensors were fabricated (under the optimal conditions) and then, they were immersed into 1.0×10^{-9} M TET solution. After that, the ΔR_{ct} was measured. The RSD was computed to be 5.6%, indicating an appropriate reproducibility of the impedimetric aptasensor.

The Aptamer/AuNPs/RGO/PGE long-term stability was also tested. Therefore, five aptasensors were prepared separately under the same conditions and stored at 4 °C for

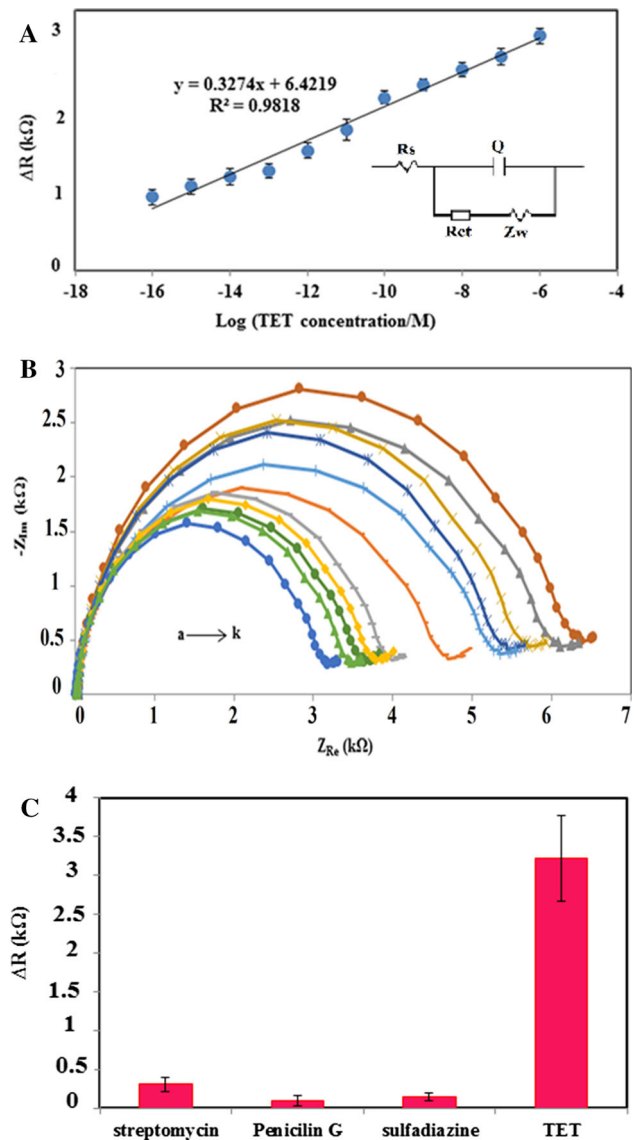


Fig. 4 a calibration plot for ΔR_{ct} versus Log concentration of TET, b Nyquist diagram for different concentration of TET, (a-k) 1.0×10^{-16} , 1.0×10^{-15} , 1.0×10^{-14} , 1.0×10^{-13} , 1.0×10^{-12} , 1.0×10^{-11} , 1.0×10^{-10} , 1.0×10^{-9} , 1.0×10^{-8} , 1.0×10^{-7} , 1.0×10^{-6} M, respectively. In 5.0 mM $\text{Fe}(\text{CN})_6^{4-3-}$ containing 0.1 M KCl solution, The error bars represented the standard deviation (SD) ($n = 3$), c Selectivity of the fabricated aptasensor ($n = 3$) with streptomycin, penicillin G and sulfadiazine instead of TET, at the same concentrations (1×10^{-9} M). The error bars represented the SD ($n = \text{three electrodes}$)

three weeks. The R_{ct} of each of them was recorded in a three-day interval. The results confirmed that 5.3% of the aptasensor efficiency was declined, indicating acceptable stability for biosensor.

For assess the aptasensor selectivity towards other antibiotics (e.g., streptomycin, penicillin G, and sulfadiazine), the ΔR_{ct} of the aptasensor was recorded using EIS method, based on the recommended procedure. The results

Table 1 Comparison of the proposed aptasensor with other methods for detection of TET

Electrode	Method	Dynamic range (M)	LOD (M)	Repeatability (RSD%)	Reproducibility (RSD%)	Stability (day)	Reference
M-shape structure of aptamer / complementary strands of aptamer/ exonuclease I/gold electrode	DPV ^a	1.5×10^{-9} – 3.5×10^{-6}	0.45×10^{-9}	7.9	8.3	–	(Taghdisi et al. 2016)
MWCNT ^b /GCE ^c	DPV	1×10^{-8} – 5×10^{-5}	5×10^{-9}	–	10	14	(Zhou et al. 2012)
Avidin-HRP ^d /bio-cDNA ^e /aptamer/ MoS ₂ -TiO ₂ @Au /GCE	DPV	1.5×10^{-10} – 6×10^{-6}	5×10^{-11}	–	5.12	10	(Tang et al. 2018)
MIP ^f /Aptamer/ AuNP/GCE	EIS	5×10^{-13} – 1×10^{-10}	144×10^{-15}	–	6.8	14	(Rad and Azadbakht 2019)
MBCPE ^g /Fe ₃ O ₄ NPs@OA ^h /anti-TET	EIS	1×10^{-14} – 1×10^{-6}	3.8×10^{-15}	–	6.8	7	(Jahanbani and Benvidi 2016)
Anti-ET/PGA ⁱ /MWCNT /GCE	DPV	1×10^{-15} – 1×10^{-6}	3.1×10^{-16}	–	5.6	7	(Benvidi et al. 2018)
TET/Aptamer/AuNPs/RGO/PGE	EIS	1×10^{-16} – 1×10^{-6}	3.05×10^{-17}	4.2	5.6	21	This work

^adifferential pulse voltammetry, ^bMulti-walled carbon nanotubes, ^cglassy carbon electrode, ^davidin-horseradish peroxidase, ^ebiotin-DNA oligonucleotide, ^fmolecular imprinted polymers, ^gmagnetic bar carbon paste, ^holeic acid, ⁱpoly L-glutamic acid

Table 2 Detection of TET in different milk samples using Aptamer/AuNPs/RGO/PGE

Sample	Spiked value (M)	Determined ^a (M)	Recovery (%)	RSD (%)
Cow milk	1×10^{-9}	$(0.942 \pm 0.057) \times 10^{-9}$	94.2	6.5
	1×10^{-11}	$(0.961 \pm 0.061) \times 10^{-11}$	96.1	6.3
Sheep milk	1×10^{-9}	$(0.928 \pm 0.071) \times 10^{-9}$	92.8	7.6
	1×10^{-11}	$(0.984 \pm 0.042) \times 10^{-11}$	98.4	4.3
Goat milk	1×10^{-9}	$(0.971 \pm 0.043) \times 10^{-9}$	97.1	4.4
	1×10^{-11}	$(0.957 \pm 0.081) \times 10^{-11}$	95.7	8.4
Water buffalo milk	1×10^{-9}	$(1.021 \pm 0.094) \times 10^{-9}$	102.1	9.2
	1×10^{-11}	$(0.977 \pm 0.010) \times 10^{-11}$	97.7	10.2

^aMean of three measurements \pm SD.

indicated that *streptomycin*, *penicillin G* and *sulfadiazine* did not interfere with TET detection. As shown in Fig. 4c, all of the tested antibiotics show much lower signal compared to TET, indicating the effective capability of the proposed aptasensor to differentiate between the target (TET) and other antibiotics. Overall, the fabricated aptasensor of TET can be utilized for quantitative and qualitative detection of TET in milk samples.

Aptasensor application in milk samples

The aptasensor's practical application was evaluated through TET detection in milk samples. The experiment was carried out into four types of milk samples. According to the response signals obtained from the aptasensor, the

recoveries were computed. As shown in Table 2, the recoveries range of the aptasensor was 92.8–102.1%. Finally, this study exhibits that the developed impedimetric aptasensor has a good accuracy and the fabricated aptasensor can be effectively utilized for the quantitative detection of TET in milk samples.

Conclusion

In the present study, a label-free aptasensor based on AuNPs/RGO nanocomposites has been successfully fabricated to quantitatively and qualitatively detect TET in milk samples. Using EIS technique, a low LOD of 3×10^{-17} , acceptable repeatability, stability, and high selectivity were

obtained for TET aptamer/AuNPs/RGO/PGE. Under optimal conditions, the TET/aptamer/AuNPs/RGO/PGE presented a broad dynamic range (1×10^{-16} – 1×10^{-6} M). The appropriate results of this research demonstrate that the proposed aptasensor is promising for TET determination and it can be potentially applied in early screening of milk samples. In general, it is suggested that the fabricated sensor be used for detection of other antibiotics in various foods such as egg, shrimp, fish, chicken, and meat.

Acknowledgement This work has been supported by the Center for International Scientific Studies & Collaboration (CISSC) and French Embassy in Iran.

References

- Ayeni FA, Odumosu BT, Oluseyi AE, Ruppitsch W (2016) Identification and prevalence of tetracycline resistance in enterococci isolated from poultry in Ilshin, Ogun State. *Niger J Pharm Bioall Sci* 8:69–73
- Benvidi A, Yazdanparast S, Rezaeinasab M, Tezerjani MD, Abbasi S (2018) Designing and fabrication of a novel sensitive electrochemical aptasensor based on poly (L-glutamic acid)/MWCNTs modified glassy carbon electrode for determination of tetracycline. *J Electroanal Chem* 808:311–320
- Chen YN, Kong DZ, Liu LQ, Song SS, Kuang H, Xu CL (2016) Development of an ELISA and immunochromatographic assay for tetracycline, oxytetracycline, and chlortetracycline residues in milk and honey based on the class-specific monoclonal antibody. *Food Anal Methods* 9:905–914
- Da Silveira VG, Oliveira MS, de Almeida CA, Hoff RB, Mallmann CA (2018) Liquid chromatography-tandem mass spectrometry determination and depletion profile of chlortetracycline, doxycycline, and oxytetracycline in broiler chicken muscle after oral administration. *Food Anal Methods* 11:2181–2194
- De los Santos Álvarez N, Abedul MTF (2020) Determination of ascorbic acid in dietary supplements by cyclic voltammetry. In: Teresa FernándezAbedul M (ed) *Laboratory Methods in Dynamic Electroanalysis*. Elsevier, Amsterdam, pp 13–23
- Ensafi AA, Akbarian F, Heydari-Soureshjani E, Rezaei B (2018) A novel aptasensor based on 3D-reduced graphene oxide modified gold nanoparticles for determination of arsenite. *Biosens Bioelectron* 122:25–31
- Hou J, Zhang H, Yang Q, Li M, Jiang L, Song Y (2015) Hydrophilic–hydrophobic patterned molecularly imprinted photonic crystal sensors for high-sensitive colorimetric detection of tetracycline. *Small* 23:2738–2742
- Izadi Z, Sheikh-Zeinoddin M, Ensafi AA, Soleimani-Zad S (2016) Fabrication of an electrochemical DNA-based biosensor for *Bacillus cereus* detection in milk and infant formula. *Biosens Bioelectron* 80:582–589
- Jahanbani S, Benvidi A (2016) Comparison of two fabricated aptasensors based on modified carbon paste/oleic acid and magnetic bar carbon paste/Fe₃O₄@ oleic acid nanoparticle electrodes for tetracycline detection. *Biosens Bioelectron* 85:553–562
- Kassaei MZ, Motamedi E, Majidi M (2011) Magnetic Fe₃O₄-graphene oxide/polystyrene: fabrication and characterization of a promising nanocomposite. *Chem Eng J* 172:540–549
- Kim YS, Kim JH, Kim IA, Lee SJ, Jung J, Gu MB (2010) A novel colorimetric aptasensor using gold nanoparticle for a highly sensitive and specific detection of oxytetracycline. *Biosens Bioelectron* 26:1644–1649
- Mohammad-Razdari A, Ghasemi-Varnamkhasti M, Izadi Z, Ensafi AA, Rostami S, Siadat M (2019a) An impedimetric aptasensor for ultrasensitive detection of *Penicillin G* based on the use of reduced graphene oxide and gold nanoparticles. *Microchim Acta* 186:372. <https://doi.org/10.1007/s00604-019-3510-x>
- Mohammad-Razdari A, Ghasemi-Varnamkhasti M, Izadi Z, Rostami S, Ensafi AA, Siadat M, Losson E (2019b) Detection of sulfadimethoxine in meat samples using a novel electrochemical biosensor as a rapid analysis method. *J Food Compos Anal* 82:103252. <https://doi.org/10.1016/j.jfca.2019.103252>
- Moreno-González D, Krulišová M, Gámiz-Gracia L, García-Campaña AM (2018) Determination of tetracyclines in human urine samples by capillary electrophoresis in combination with field amplified sample injection. *Electrophoresis* 39:608–615
- Moudgil P, Bedi JS, Aulakh RS, Gill JPS, Kumar A (2019) Validation of hplc multi-residue method for determination of fluoroquinolones, tetracycline, sulphonamides and chloramphenicol residues in bovine mil. *Food Anal Methods* 12:338–346
- Niu X, Li X, Chen W, Li X, Weng W, Yin C, Li G (2018) Three-dimensional reduced graphene oxide aerogel modified electrode for the sensitive quercetin sensing and its application. *Mater Sci Eng C* 89:230–236
- Ouyang Q, Liu Y, Chen Q, Guo Z, Zhao J, Li H, Hu W (2017) Rapid and specific sensing of tetracycline in food using a novel upconversion aptasensor. *Food Control* 81:156–163
- Palamy S, Ruengsitagoon W (2017) A novel flow injection spectrophotometric method using plant extracts as green reagent for the determination of doxycycline. *Spectrochim Acta A Mol Biomol Spectrosc* 171:200–206
- Rad AO, Azadbakht A (2019) An aptamer embedded in a molecularly imprinted polymer for impedimetric determination of tetracycline. *Microchim Acta*. <https://doi.org/10.1007/s00604-018-3123-9>
- Rezaei B, Jamei HR, Ensafi AA (2018) An ultrasensitive and selective electrochemical aptasensor based on rGO-MWCNTs/Chitosan/carbon quantum dot for the detection of lysozyme. *Biosens Bioelectron* 115:37–44
- Shen L, Chen J, Li N, He P, Li Z (2014) Rapid colorimetric sensing of tetracycline antibiotics with in situ growth of gold nanoparticles. *Anal Chim Acta* 839:83–90
- Shi L, Rong X, Wang Y, Ding S, Tang W (2018) High-performance and versatile electrochemical aptasensor based on self-supported nanoporous gold microelectrode and enzyme-induced signal amplification. *Biosens Bioelectron* 102:41–48
- Song Y, Luo Y, Zhu C, Li H, Du D, Lin Y (2016) Recent advances in electrochemical biosensors based on graphene two-dimensional nanomaterials. *Biosens Bioelectron* 76:195–212
- Taghdisi SM, Danesh NM, Ramezani M, Abnous K (2016) A novel M-shape electrochemical aptasensor for ultrasensitive detection of tetracyclines. *Biosens Bioelectron* 85:509–514
- Tang Y, Liu P, Xu J, Li L, Yang L, Liu X, Zhou Y (2018) Electrochemical aptasensor based on a novel flower-like TiO₂ nanocomposite for the detection of tetracycline. *Sens Actuators B* 258:906–912
- Tang YB, Lee CS, Xu J, Liu ZT, Chen ZH, He Z, Luo L (2010) Incorporation of graphenes in nanostructured TiO₂ films via molecular grafting for dye-sensitized solar cell application. *ACS Nano* 4:3482–3488
- Tian L, Qian K, Qi J, Liu Q, Yao C, Song W, Wang Y (2018) Gold nanoparticles superlattices assembly for electrochemical biosensor detection of microRNA-21. *Biosens Bioelectron* 99:564–570
- Wang N, Lin M, Dai H, Ma H (2016) Functionalized gold nanoparticles/reduced graphene oxide nanocomposites for ultrasensitive electrochemical sensing of mercury ions based on

- thymine–mercury–thymine structure. *Biosens Bioelectron* 79:320–326
- Wu L, Lu X, Fu X, Wu L, Liu H (2017) Gold nanoparticles dotted reduction graphene oxide nanocomposite based electrochemical aptasensor for selective, rapid, sensitive and congener-specific PCB77 detection. *Sci Rep* 7:5191
- Zhang Y, Yan X, Yan Y, Chen D, Huang L, Zhang J, Tan S (2018) The utilization of a three-dimensional reduced graphene oxide and montmorillonite composite aerogel as a multifunctional agent for wastewater treatment. *RSC Adv* 8:4239–4248
- Zhou L, Li DJ, Gai L, Wang JP, Li YB (2012) Electrochemical aptasensor for the detection of tetracycline with multi-walled carbon nanotubes amplification. *Sens Actuators B* 162:201–208

Publisher's Note Springer Nature remains neutral with regard to jurisdictional claims in published maps and institutional affiliations.